CHAPTER III

HEAT TRANSFER MECHANISM OF A SINGLE HEAT PIPE

In this chapter, the heat transfer processes in the evaporator and condenser and the associated temperature drops in a heat pipe will be considered. The temperature drops can be represented by thermal resistances. The heat transfer mechanism and correlations for predicting the heat transfer coefficients in both sections will also be discussed.

3.1 The Thermal Resistance in Heat Pipe.

The primary heat transfer mechanism in a heat pipe consists of the following step (1):

1. Heat convection from a heat source to the pipe wall
2. Heat conduction across the pipe wall
3. Boiling heat transfer of a liquid pool and evaporation from the film surface in the evaporator.
4. Axial convective heat transfer by vapor from the evaporator to the condenser section.
5. Vapor condensation onto a liquid film in the condenser.
6. Heat conduction across the pipe wall at the condenser.
7. And finally heat convection to the external heat sink.

The heat flow paths of a closed two-phase thermosyphon and the equivalent thermal resistance in each section is shown in Figure 3.1.

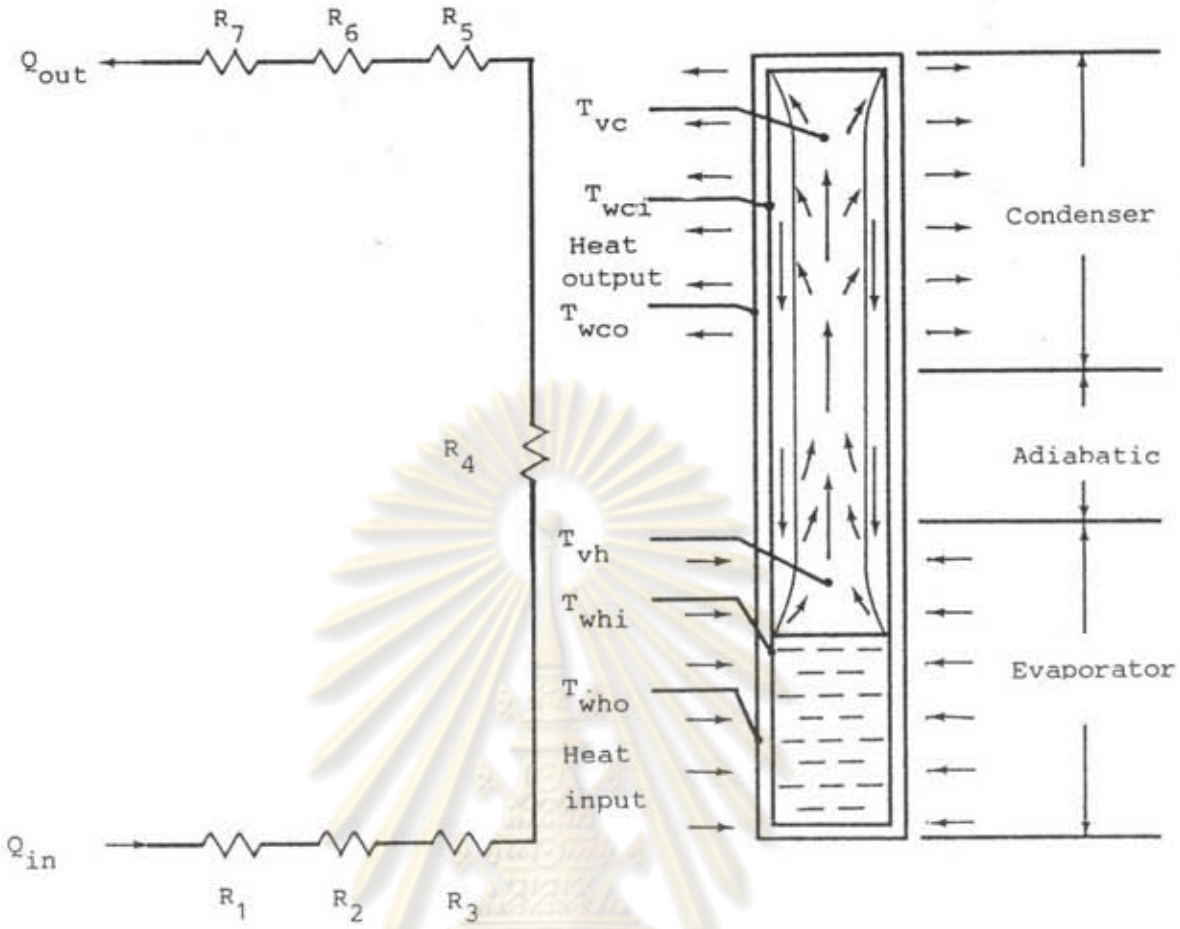

Figure 3.1 Sketch of heat flow paths and equivalent thermal resistances of a thermosyphon.

For steady-state operation, the heat transfer rate can be calculated by the following equation (33):

$$Q_p = \frac{1}{R_t}(T_h - T_c) \tag{3.1}$$

$$= \frac{1}{R_1}(T_h - T_{who}) \tag{3.2}$$

$$= \frac{1}{R_2}(T_{who} - T_{whi}) \tag{3.3}$$

$$= \frac{1}{R_3}(T_{whi}-T_{vh}) \tag{3.4}$$

$$= \frac{1}{R_4}(T_{vh}-T_{vc}) \tag{3.5}$$

$$= \frac{1}{R_5}(T_{vc}-T_{wci}) \tag{3.6}$$

$$= \frac{1}{R_6}(T_{wci}-T_{wco}) \tag{3.7}$$

$$= \frac{1}{R_7}(T_{wco}-T_c) \tag{3.8}$$

where

$$R_t = \sum_{i=1}^{7} R_i \tag{3.9}$$

$$R_1 = \frac{1}{h_{oh}A_{oh}} \tag{3.10}$$

$$R_2 = \frac{\ln (r_o/r_i)}{2\pi k L_h} \tag{3.11}$$

$$R_3 = \frac{1}{h_{ih}A_{ih}} \tag{3.12}$$

$$R_4 = \frac{F_v[(1/6)L_h + L_a + (1/6)L_c]T_v}{\rho_v \lambda J} \tag{3.13}$$

where F_v = frictional coefficient for vapor flow

$$= \frac{(f_v Re_v)\,\mu_v}{2r^2_{h,v}A_v\,\rho_v\,\lambda}$$

$$R_5 = \frac{1}{h_{ic}A_{ic}} \tag{3.14}$$

ศูนย์วิทยทรัพยากร
จุฬาลงกรณ์มหาวิทยาลัย

$$R_6 = \frac{\ln(r_o/r_i)}{2\pi k L_c} \tag{3.15}$$

$$R_7 = \frac{1}{h_{oc} A_{oc}} \tag{3.16}$$

R_1, R_7 is the convection film heat transfer resistances around the evaporator and condenser, respectively, and can be calculated by, says, the correlation of Sieder and Tate (40) for forced convection of laminar flow in the pipe.

$$Nu = 1.86\ Re^{1/3} Pr^{1/3} (L/D)^{-1/3} (\mu_b/\mu_w) \tag{3.17}$$

where the physical properties of the fluid are evaluated at the mean bulk temperature.

R_2,R_6 represent the thermal resistances of the heat pipe wall, calculated by Fourier's law of heat conduction for a cylindrical wall.

R_3,R_5 are the thermal resistances of the evaporation and condensation processes in a heat pipe. The heat transfer correlations for these processes will be described in the next sections.

R_4 is the thermal resistance due to the temperature drop along the vapor column and can be calculated by the Clausius-Clapeyron (1) equation, which relates the vapor temperature and pressure as follows:

$$T_1 - T_2 = \frac{T_v\ (P_1 - P_2)}{\rho_v\ J} \tag{3.18}$$

Generally R_4 is very small and can be neglected.

3.2 Heat Transfer Processes in the Evaporator

The evaporation in the evaporator could be arranged in order as (41) :

1. the evaporation from the free surface of liquid pool

2. the direct evaporation in the liquid pool, namely, the boiling which includes nucleate boiling at a light thermal load and film boiling at a heavy thermal load.

The returning condensate from the condenser to the evaporator could be catagorized into the following forms as reported by Andros and Florschuetz (42).

1. a smooth continuous film with surface evaporation

2. the breakdown of the smooth continuous film into a series of stable rivulets

3. a wavy film with unstable rivulets

4. a wavy film with bubble nucleation occurring in the unstable rivulets

The occurrence of these different flow patterns of the condensate depends on the difference of the surface tensions and contact angle of the working fluid to the container material. The surface tensions and contact angle usually vary with the temperature, so the behavior of the condensate in the evaporator is quite complex.

Due to the complexity of the heat transfer mechanism in the evaporator, the correlations for predicting the heat transfer coefficients in the whole evaporator section are still unavailable. The nucleate boiling in the liquid pool is generally considered as the dominant phenomena in the evaporator, so the nucleate boiling behavior and correlation will be summarized first and then followed by the correlations for evaluating the heat transfer coefficients in the

evaporator proposed by some investigators in the literature.

3.2.1 The Boiling Heat Transfer from Plane Surfaces (43)

Consider a plane heater immersed in a pool of liquid, which is maintained at a temperature T_s, the boiling point corresponding to the pressure of the system. Let T_w be the temperature of the heater surface. Figure 3.2 shows how the heat flux q will vary with $T_w - T_s$ as the heater power is raised. This curve was first obtained by Nukiyama for water and it is found that all liquids behave in a similar way.

The region A-B corresponds to natural convection to the evaporating surface.

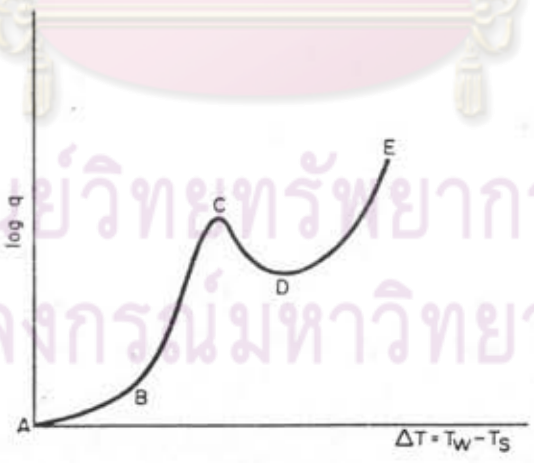

Figure 3.2 Pool boiling regimes

ศูนย์วิทยทรัพยากร
จุฬาลงกรณ์มหาวิทยาลัย

As the flux increases bubbles form at the surface and very high heat transfer rates can be achieved with quite small temperature differences. This region B-C is known as the nucleate boiling or pool boiling region. The bubbles both transport heat by latent heat and also increase convective heat transport.

The heat flux in nucleate boiling cannot be increased indefinitely, at point C the bubble population becomes so high that it becomes difficult for the liquid to reach the heater surface and a continuous vapor film forms. The temperature difference increases rapidly and the condition is known as burnout, boiling crisis, or critical heat flux. The region C-D is known as the partial film boiling region, boiling is unstable and the surface is alternately covered by vapor and liquid. From D-E the vapor film is stable and the condition called stable film boiling. The point E is determined by the melting point of the heater material.

3.2.1.1 Nucleate Boiling and Bubble Formation

Equation (3.19) shows that the pressure difference across a curved surface radius r is given by

$$P = \frac{2\sigma}{r} \qquad (3.19)$$

For a bubble to form it must start at a nucleation center which provides a finite initial radius. In addition the liquid must be superheated in order to provide the pressure difference ΔP.

The amount of required superheat ΔT_s may be related to ΔP by the Clausius-Clapeyron equation:

$$\frac{dP}{dT} = \frac{1}{T\ (V_v - V_l)} \tag{3.20}$$

where V_v is the volume of unit mass of the vapour

V_l is the volume of unit mass of the liquid

Normally $V_l << V_v$

Hence $$\frac{dP}{dT} = \frac{\lambda}{T\ V_v}$$

Combining equations (3.19) and (3.20)

$$\Delta T = \frac{2\ 6\ TV_v}{\lambda\ r} = \frac{2\ 6\ T}{\rho_v\ \lambda\ r} \tag{3.21}$$

ศูนย์วิทยทรัพยากร
จุฬาลงกรณ์มหาวิทยาลัย

The mechanism of bubble formation depends strongly on the wetting characteristics of the heating surface. The effect of wetting on bubble formation is shown in Figure 3.3 a. Bubbles form most readily if the surface is nonwetting. In addition to wetting, nucleation sites are necessary for bubble formation.

Nucleation sites are provided by scratched or rough surfaces and by the release of absorbed gas. Figure 3.3 b shows how a bubble

form in a crevasse in a surface. As might be expected, a much higher superheat is required to form bubbles on a clean, smooth surface. Figure 3.4 shows how the temperature varies with distance from the surface, under nucleate boiling conditions, for the case of water on stainless steel at atmospheric pressure. Schins (43) reported similar measurements for sodium boiling at 785°C - 875°C in a stainless steel boiler. Schins found that due to the wetting of stainless steel by sodium, nucleation was difficult to start and a superheat of 100°C was required. After some time the surface became conditioned and superheat dropped to around 20°C. This result is surprising since one might have expected reverse behaviour.

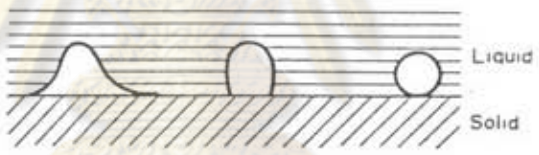

(i) No wetting (ii) Partial wetting (iii) Complete wetting

(a) Effect or wetting

(b) Bubble formation at a crevasse nucleation site

Figure 3.3 Bubble formation on a heated surface

ศูนย์วิทยทรัพยากร
จุฬาลงกรณ์มหาวิทยาลัย

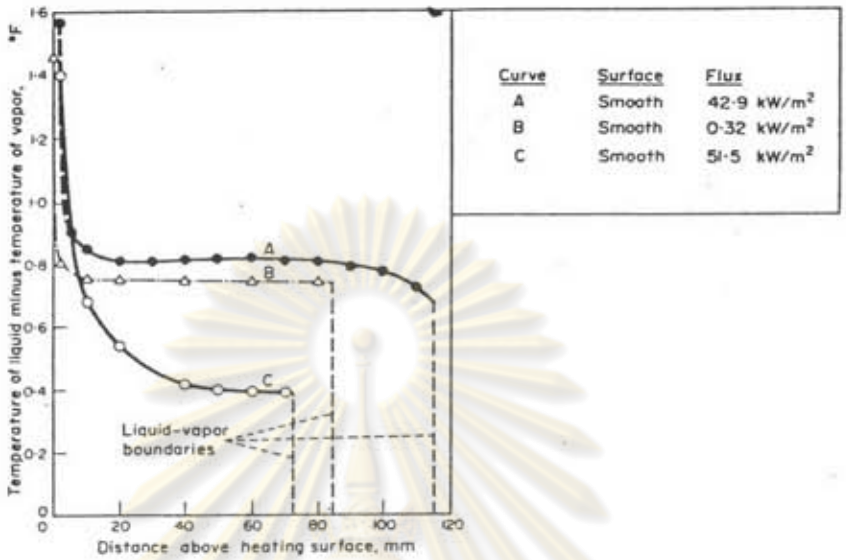

Figure 3.4 Variation of temperature with distance from a surface under nucleate boiling considerations

Hsu (43) has obtained an expression similar in form to equation (3.21).

$$T = \frac{12.8\ \delta\ T_s}{J\ \rho_v\ \lambda\ \delta} \qquad (3.21)$$

$$= \frac{3.06\ \delta\ T_s}{\rho_v\ \lambda\ \delta} \quad \text{in S.I. units} \qquad (3.22)$$

where δ is the thermal layer thickness. As a first approximation this may be taken as the average diameter of cavities on the surface. For typical surfaces this is around 10^{-3} inches or 2.5×10^{-3} cm.

Table 3.1 Superheat ΔT calculated for some liquids, at their boiling points at atmospheric pressure, using Hsu's formula

Fluid	Boiling point K	Vapour density kg/m^3	Latent heat kJ/kg	Surface tension N/M	T ^oC
Ammonia (NH_3)	239.7	0.3	1350	0.028	2.0
Ethyl alcohol	338	2.0	840	0.021	0.51
Water	373	0.60	2258	0.059	1.9
Potassium	1047	0.486	1938	0.067	8.9
Sodium	1156	0.306	3913	0.113	26.4
Lithium	1613	0.057	19700	0.26	44.8

3.2.1.2 Correlation of nucleate boiling data

Nucleate boiling is very dependent on the heated surface and factors such as release of absorbed gas, surface roughness, surface oxidation and wettability greatly affect the surface to bulk liquid temperature difference. The nature of the surface may change over period of time - a process known as conditioning. (The effect of pressure is also important.) For these reasons reproducibility of results is often difficult. However a number of authors have proposed correlations, some empirical and some based on physical models.

3.2.1.3 Nucleate boiling in water and organic liquids

A useful correlation applicable to these fluids has been attained by Rohsenhow (43). In his model Rohsenhow considered the convective heat transfer due to bubbles.

From dimensional considerations

$$Nu = f(Re_b, Pr_l)$$

where Nu_b is the Nusselt number for bubble and is the ratio of heat transferred by convection q to that transmitted by conduction $k\Delta T$.

$$\text{i.e } Nu = \frac{q}{k\Delta T}$$

Pr_l is the Prandtl Number for the liquid and is defined as $(C_p \mu)/k$, the ratio of the kinematic to the thermal diffusivity

Re_b is the Reynolds number for the bubble

$= \dfrac{\rho_v V_l D_l}{\mu}$ where D_l is the bubble diameter

Rohsenhow extended this relation empirically and found

$$\frac{Re_b Pr_l}{Nu_b} = C\, Re_b^{\,n}\, Pr_e^{\,m}$$

Using a 0.024-inch platinum wire in distilled water, he obtained the relation

$$\frac{C_p \Delta T}{\lambda} = 0.013 \left[\frac{q}{\lambda\mu}\sqrt{\frac{g_c\, \sigma}{g\ \ (\rho - \rho_v)}}\right]^{0.33} \left[\frac{C_p \mu}{k}\right]^{1.7} \qquad (3.23)$$

The term g/g_c is the gravitational acceleration referred to the standard value $g_c = 9.81\ m/s^2$ and is required for example in space applications.

The Rohsenhow correlation agrees well with data from other fluid-surface combinations if the constant 0.013 is replaced by values listed in Table 3.2.

A number of authors have provided relationships to enable the critical heat flux q_{cr} to be predicted.

One of these was developed by Rohsenhow and Griffith (43) who obtained the following expression

$$\frac{q_c}{\lambda \rho_v} = 0.012 \left[\frac{\rho - \rho_v}{\rho_v}\right]^{0.6} \qquad (3.24)$$

Another correlation due to Caswell and Balzhieser (43) applies to both metals and non-metals.

$$\frac{q\ C_p^{r}}{\lambda^2 \rho_v k}\ Pr^{-0.71} = 1.02 \times 10^{-6} \left[\frac{\rho - \rho_v}{\rho_v}\right]^{0.65} \qquad (3.25)$$

Other comprehensive references on liquid-metal boiling are given by Subbotin and Dwyer.

ศูนย์วิทยทรัพยากร
จุฬาลงกรณ์มหาวิทยาลัย

i17419503

Table 3.2 Correlation of Equation (3.23) with r = 0.33

Surface fluid combination	°C
Water-nickel	0.006
Water-platinum	0.013
Water-copper	0.013
Water-brass	0.006
Water-nickel and stainless steel	0.013
Water-stainless steel	0.014
Carbon tetrachloride-copper	0.013
Benzene-chromium	0.010
n-pentane-chromium	0.015
Ethyl alcohol-chromium	0.0027
Isopropyl alcohol-copper	0.0025
35% K_2CO_3-copper	0.0054
50% K_2CO_3-copper	0.0027
n-butyl alcohol-copper	0.0030

ศูนย์วิทยทรัพยากร
จุฬาลงกรณ์มหาวิทยาลัย

3.2.2 Correlations of Evaporator Heat Transfer Coefficients

M, Shiraishi and et al.(42) proposed two correlations for calculating the heat transfer coefficients in the liquid pool and liquid film separately.

In the liquid pool, the heat transfer process was thought to be the same as the boiling heat transfer in an open thermosyphon except for the operating pressure. The heat transfer coefficient of the boiling in thermosyphon was given by

$$h_p(\text{closed}) \propto h_p(\text{open})(P/P_a)^m \tag{3.26}$$

Where P_a is the atmospheric pressure and h_p(open) is the boiling heat transfer coefficient in the open thermosyphon calculated from the empirical correlation of Kusuda and Imura (42). Then the heat transfer coefficient of the boiling in the two-phased closed thermosyphon was obtained as follows

$$h_p = \frac{0.32\,\rho^{0.65}k^{0.3}C_p^{0.7}g^{0.2}(P/P_a)^{0.23}q_h^{0.4}}{\rho_v^{0.25}\,\lambda^{0.4}\,\mu^{0.1}} \tag{3.27}$$

For heat transfer in the liquid film, the continuous liquid film was observed at low evaporator heat flux so the laminar film evaporation model which is the reverse of Nusselt's condensation theory was applied. At high evaporator heat flux mathematical model in this region is not possible at present due to the complexity of the mechanism. However they considered that the heat transfer coefficient was approximated by the above boiling in the liquid pool and the heat transfer coefficient of the liquid film in the evaporator section was given by

$$\frac{h_f(\nu^2/g)^{1/3}}{k} = (4/3)^{1/3}Re_f^{-1/3} \tag{3.28}$$

$$= h_f^* \qquad ; \quad q_h < q_h^*$$

$$h_f = h_p \qquad ; \quad q_h > q_h^*$$

Where $Re_f = (4xq_h)/(\lambda\mu)$

$$x = L_p + 0.5\,L_f \tag{3.29}$$

Kobayashi (44) proposed a model of the working flow pattern and heat transfer mechanism which segregated into 5 regions in the evaporator: natural convection region, forced convection region, boiling region, forced convection and boiling region and vapor flow region. Each region was considered uniform with the working fluid flowing down at contact width and the heat transfer coefficient in each region was calculated from the following expressions:

1. For natural convection region, they assumed that the heated inner surface of the heat pipe was the horizontal flat plate.

$$Nu = 0.54\ (Gr\ .\ Pr)^{1/4} \quad \text{for laminar flow} \tag{3.30}$$

$$Nu = 0.14\ (Gr\ .\ Pr)^{1/3} \quad \text{for turbulent flow} \tag{3.31}$$

2. For forced convection region, they also assumed that the heated surface was horizontal flat plate.

$$Nu = 0.332\ Re^{1/2} Pr^{1/3} \tag{3.32}$$

$$Nu = 0.0296\ Re^{0.8} Pr^{1/3} \tag{3.33}$$

3. For boiling region, the empirical correlations of the heat transfer coefficients of Freon at a high superheated area and low superheated area proposed by Nishikawa and et al (44) were used.

$$h_l = 71.13\ f_l^{\,3} f_s^{\,2}\ \Delta T^2 \tag{3.34}$$

$$h_h = 5.824\ f_h^{\,5} f_s^{\,4}\ \Delta T^4 \tag{3.35}$$

for Freon 113

$$\Delta T_t = 3.4947\ f_t/f_s$$

$$f_l = P_r^{0.19}(1+2P_r^2+7P_r^8)$$

$$f_h = P_r^{0.23}(1+3P_r^2+8P_r^8)$$

$$f_t = f_l^{1.5}/f_h^{2.5}$$

Here ΔT_{bo} is the superheated of critical heat flux

P_r is reduced pressure and f_s is foamability usually equal to 1 - 3.6

4. For forced convection and boiling region. In the region where forced convection and boiling occur simultaneously, the heat transfer coefficient was estimated using the well-known proposed by Clark-Rohsenow.

$$h = h_{conv} + h_{boil} \tag{3.36}$$

Where h_{conv} = heat transfer coefficient of forced convection without boiling

h_{boil} = heat transfer coefficient of natural convective boiling

5. For vapor flow region. The vapor flow region was divided into a laminar flow region and turbulent flow region. The following Graetz's equations for laminar flow (3.37, 3.38) and Dittus-Boelter's equation for turbulent flow were used.

$$Nu = 1.75\left[\frac{\pi dRePr}{4\ L}\right]^{1/3} \tag{3.37}$$

laminar: Re < 2000

in the inlet length of temperature Gz > 10

Or $$Nu = 3.65 \tag{3.38}$$

laminar: Re < 2000

out of the inlet length of temperature Gz < 10

$$Nu = 0.023\ Re^{0.8}\ Pr^{0.4} \tag{3.39}$$

turbulent $Re > 2300$

The calculated values from this model were in good agreement with the experimental results and the proportion of heat transport in each region at tilt angle of 1, 45 and 90 degrees, under the condition of vapor temperature of 55°C and hot water temperature of 85°C, verified that the heat transport by boiling formed 70-90 % of the overall heat transport.

Wen Yaopu and Guo Shun (23) conducted experiments on the water, acetone and Freon-12 in the range of heat input from 0.5 to 16 W/cm^2 and found that the heat transfer coefficients are close to that of the liquid pool given by the Knudzilin relation. The empirical correlation obtained are presented as follows.

$$h_h/h_p = 2.35\ (P_s/P_{cr})^{0.14} \tag{3.40}$$

where h_h is evaporator heat transfer coefficient

h_p is boiling coefficient taken from the Knudzilin relation.

$$Nu = 0.082\ Pr^{-0.45} Kq^{0.7} Ku^{1/3} \tag{3.41}$$

where $Nu = \dfrac{dh_p}{k}$

$$Pr = \frac{C_p \mu}{k}$$

$$Kq = \frac{\lambda \rho_v q}{T_s k\ (\rho - \rho_v) g}$$

$$Ku = \frac{T_s C_p \sigma \rho}{\lambda^2 \rho_v^2 d}$$

$$d = \text{dimensionless number}$$

$$= \left[\frac{\sigma}{g(\rho - \rho_v)}\right]^{1/2}$$

The thermal properties of the working fluid are taken at the saturated temperature. The ratios h_h/h_p for the three working fluids are

water : 0.7-1.5

acetone : 1.05-1.5

F12 : 1.4-2.5

3.3 Heat Transfer in the Condenser

Vapor will condense on the liquid surface in the condenser and there will be a small temperature drop and hence thermal resistance. Condensation phenomena in the condenser is not so complex as the evaporator in practice. Condensation can occur in two forms, either by the condensing vapor forming a continuous liquid surface or by forming a large number of drops, which depend on the combination of the working fluid and the container material. Film condensation generally occurs in thermosyphon and will be described here. However in the heat pipe, vapor pumping will cause such gas to be concentrated at the end of the condenser. This part of the condenser will be effectively shut off and this effect is the basis of the gas buffered heat pipe.

The first analysis of film condensation is due to Nusselt and is given in the standard text books. The theory considers condensation

onto a vertical surface and the resulting condensed liquid film flows down the surface under the action of gravity and the flow is assumed to be laminar. Viscous shear between the vapor and liquid phase is neglected. The mass flow increases with distance from the top and the flow profile is shown in Figure 3.5.

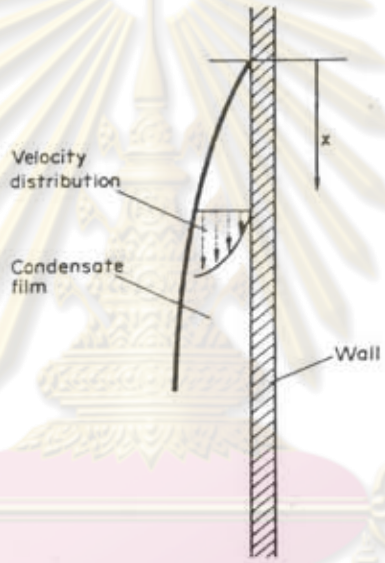

Figure 3.5 Film condensation on a vertical surface

The average heat transfer coefficient h over a distance x from the top is given by

$$h = 0.943 \left[\frac{\lambda \rho^2 g k^3}{x \mu (T_s - T_w)} \right]^{1/4} \qquad (3.42)$$

where $T_s - T_w$ is the difference in temperature across the film.